THE JOURNAL OF PHYSICAL CHEMISTRY LETTERS
A JOURNAL OF THE AMERICAN CHEMICAL SOCIETY

pubs.acs.org/JPCL

Letter

# Direct Observation of Single-Protein Transition State Passage by Nanopore Ionic Current Jumps

Prabhat Tripathi, Arash Firouzbakht, Martin Gruebele,* and Meni Wanunu*

Cite This: *J. Phys. Chem. Lett.* 2022, 13, 5918−5924

Read Online

ACCESS | Metrics & More | Article Recommendations | Supporting Information

**ABSTRACT:** Conformational transitions of proteins are governed by chemical kinetics, often toggled by passage through an activated state separating two conformational ensembles. The passage time of a protein through the activated state can be too fast to be detected by single-molecule experiments without the aid of viscogenic agents. Here, we use high-bandwidth nanopore measurements to resolve microsecond-duration transitions that occur between conformational states of individual protein molecules partly blocking pore current. We measure the transition state passage time between folded and unfolded states of a two-state $\lambda_{6-85}$ mutant and between metastable intermediates and the unfolded state of the multistate folder cytochrome *c*. Consistent with the principle of microscopic reversibility, the transition state passage time is the same for the forward and backward reactions. A passage time distribution whose tail is broader than a single exponential observed in cytochrome *c* suggests a multidimensional energy landscape for this protein.

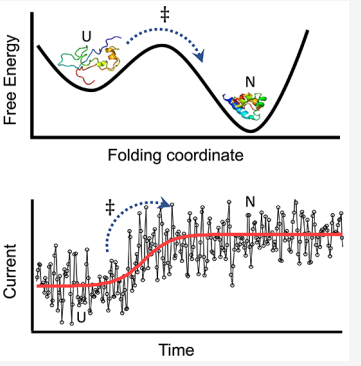




As in the case of elementary chemical reactions, protein folding is typically represented by a free energy landscape, on which sequential protein conformational transitions correspond to saddle points.[1] When approximated by Kramers' theory,[2] the reaction rate can be split into a prefactor and a Boltzmann factor that depend on the activation free energy. Unlike isomerization or bond-cleaving reactions of small molecules, where the prefactor has been measured in the subpicosecond range,[3] the transition state passage of proteins is limited by chain diffusion within 1 $k_BT$ of the saddle point[4] and occurs on a slower, up to microseconds, time scale. Nonetheless, these fleeting moments when a biomolecular reaction actually occurs are difficult to capture.

The passage time defines the "speed limit" for folding, with an early estimate of ∼1 $\mu$s based on chain rearrangement of denatured cytochrome *c*.[5] Ensemble experiments on proteins engineered to fold very quickly have reached this time scale:[6] linear response theory[7] predicts that for barriers approaching 1 $k_BT$ the ensemble signature for transition state passage is as a fast "molecular phase" preceding the activated kinetics, which has been measured for several proteins with fast folding times.[8,9] Such proteins are termed "downhill folders"[10] or "incipient downhill folders" if the barrier is near 1 $k_BT$ but not zero.[11]

Single-molecule fluorescence[12] and optical tweezers[13] experiments have been performed as well to measure the transition state passage time of proteins and RNAs, observing it in the presence of viscogens to slow down diffusion or during force extension of the amino acid chain.[13,14] Extrapolation of single-molecule experiments of slower folding proteins to zero viscogen concentration[12] agrees well with ensemble experiments of proteins engineered to fold quickly.[11] Current single-molecule fluorescence methods necessarily require additives (viscogens or denaturants) as well as dye labeling to achieve the required experimental conditions, whereas force experiments do not directly probe the same reaction coordinate as of spontaneous folding/unfolding. The full resolution of transition path time for single unlabeled biomolecules under folding conditions thus remains a challenging task.

Here we use a method complementary to fluorescence or force measurements—high-bandwidth measurement of ionic current through a solid state nanopore—to monitor the transition state passage of single-protein molecules without denaturing or viscogenic additives, mechanical force, or chemical labeling. An electric field holds a single charged protein near a nanopore by voltage application across the pore.[15] The voltage induces an ion current through the pore that probes the protein conformation with submicrosecond time resolution. When the protein switches conformation, the ion current jumps, and if the current jump can be resolved, the transition state passage time can be resolved. Eventually the protein translocates through the pore, yielding maximum ion current. The translocation cycle ends by another protein settling on the pore.

**Received:** April 6, 2022
**Accepted:** June 17, 2022




https://doi.org/10.1021/acs.jpclett.2c01009
*J. Phys. Chem. Lett.* 2022, 13, 5918−5924

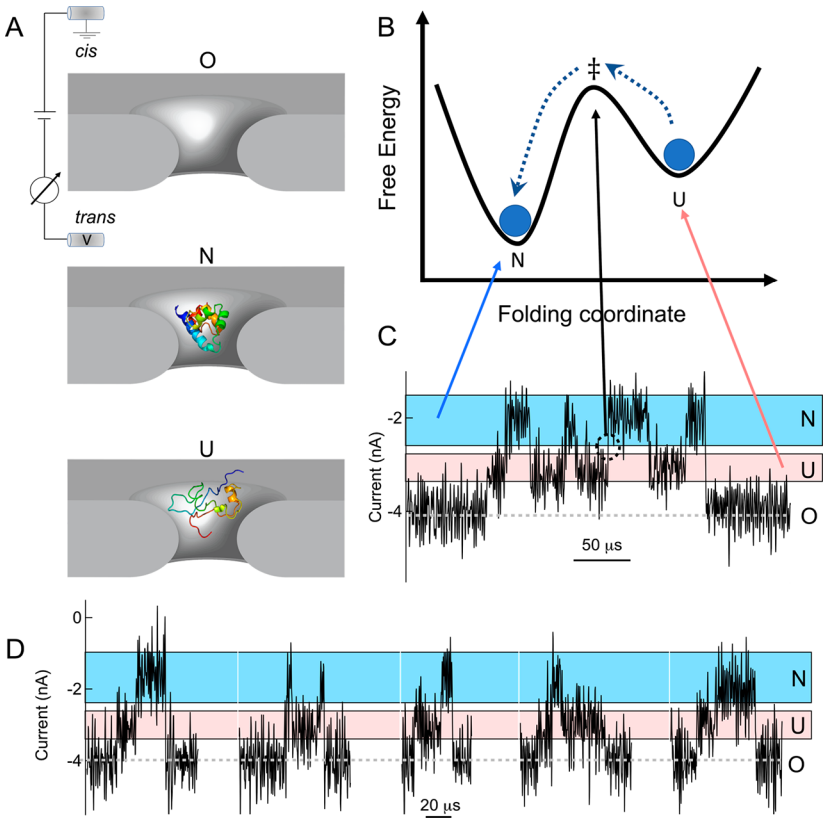


**Figure 1.** Schematic of transition state between the folding to unfolding transition in a two-state N27C mutant of the λ-repressor family. (A) Application of voltage in the trans chamber electrokinetically captures the protein molecules undergoing dynamic equilibrium between native (N) and unfolded states (U). (B) Potential energy surface for the folding reaction coordinate. (C) Example ionic current trace recorded with a 4 nm pore where activated state between U → N and N → U transitions can be directly observed. The dotted circle and black arrow from (C) to (B) highlights a transition state passage event. (D) Several more current transients showing both arrival of protein, conformational transitions, and finally translocation to restore an open (O) pore.

We observe the transition state passage of two protein molecules: a fast two-state folding mutant of λ-repressor fragment $\lambda_{6-85}$, with a low barrier previously estimated to be ∼4.5 $k_BT$,[16] and the slow multistate folder cytochrome *c* (cyt *c*) with a free energy barrier for unfolding previously estimated to be >21 $k_BT$.[17] Our single-molecule experiments capture the transition state dynamics for both the forward and backward reactions independently for dozens of events for each protein. The average forward and backward transition state passage times are the same, in agreement with the principle of microscopic reversibility, as observed previously in experiments slowing the transition with viscogens.[12] In addition, we find that the transition state passage time is not measurably affected by the strength of the electric field, suggesting that the transition state dynamics is not strongly coupled to the translocation. The average transition state passage time of the λ-repressor mutant is ∼0.4 μs, and that of cyt *c* for passage between two different pairs of states is ∼0.5 and 3 μs, consistent with the expected speed limit extrapolated from high temperature to room temperature in ensemble experiments,[9] the original speed limit estimation based on chain rearrangement in denturant,[5] estimates based on molecular dynamics simulations, and single-molecule fluorescence measurements in viscogens.[12]

A schematic of our experimental setup is shown in Figure 1A. Previous reports[18,19] demonstrated the ability of solid state nanopores to observe ionic current jumps occurring on the microseconds time scale by using a custom voltage sensor (Chimera VC 100). This instrument can measure the ionic current through the nanopore at 4.17 MHz sampling frequency (∼240 ns sampling time resolution of the instrument). We formed a nanoscale pore on an insulating SiN membrane,[18−20] which separates two compartments, *cis* and *trans*, each containing the same electrolyte buffer solution (1 M KCl in 10 mM HEPES, pH 7.5). We keep protein concentration low, so proteins diffuse to the pore at a much lower rate (<25 $s^{-1}$) than the observed folding, unfolding, or translocation rates. Application of an electric potential on the *trans* side, while keeping the *cis* side grounded, generates an ionic current through the pore that is reduced while a single-protein molecule resides near the pore. As described previously,[15] for sufficiently small pores (<4 nm), the ionic current reduction is greater for a folded protein (N state) in comparison to the more permeable unfolded protein (U state). Thus, toggling of the ionic current signature while a single protein interconverts between folded, intermediate, and unfolded states at the nanopore yields information about the forward and backward transition state passage as illustrated in Figure 1B. Figure 1C illustrates an example of the nanopore ionic current signature for several reversible folding and unfolding events, which occur after a single protein settles on the pore and before the single-protein molecule translocates through the pore or retracts back to *cis*.

Consistent with the energy landscape theory picture, prior single-molecule fluorescence experiments suggested that a fast and a slow-folding protein take almost the same time to pass



https://doi.org/10.1021/acs.jpclett.2c01009
J. Phys. Chem. Lett. 2022, 13, 5918−5924

from the folded to unfolded state (i.e., two proteins with folding/unfolding rate coefficients that differ by >1000-fold take almost the same time to pass through transition state).[12] Earlier experiments in bulk solution also indicate a similar speed limit of folding for the folding/unfolding reaction of λ-repressor and cyt *c* protein systems.[5,8] To demonstrate this principle, we used two different protein systems—a fast-folding λ-repressor mutant ("N27C")[8,21] and cytochrome *c*[5,17]—to measure the transition state passage time in single-molecule nanopore experiments. While N27C and cyt *c* are similar in size ($d_{protein}$ ~ 3 nm), their folding dynamics are different: the N27C mutant folds in a single step and has an ~1000 times faster folding rate coefficient than cyt *c*,[17] which folds in several steps.

The two-state nature of the N27C folding transition makes it an ideal candidate for directly observing the transition state passage on a microseconds time scale during the folding of a label-free single molecule. Nanopores smaller than the size of the protein only allow the passage of the protein in its metastable intermediate and unfolded conformational states.[15] Thus, for the two-state N27C protein we used a pore of diameter (4 nm) slightly larger than the protein to observe the transition between folded and unfolded states. Example ionic current traces for the interaction of the N27C mutant with a 4 nm pore are shown in Figure 2 and more in Figure S1.

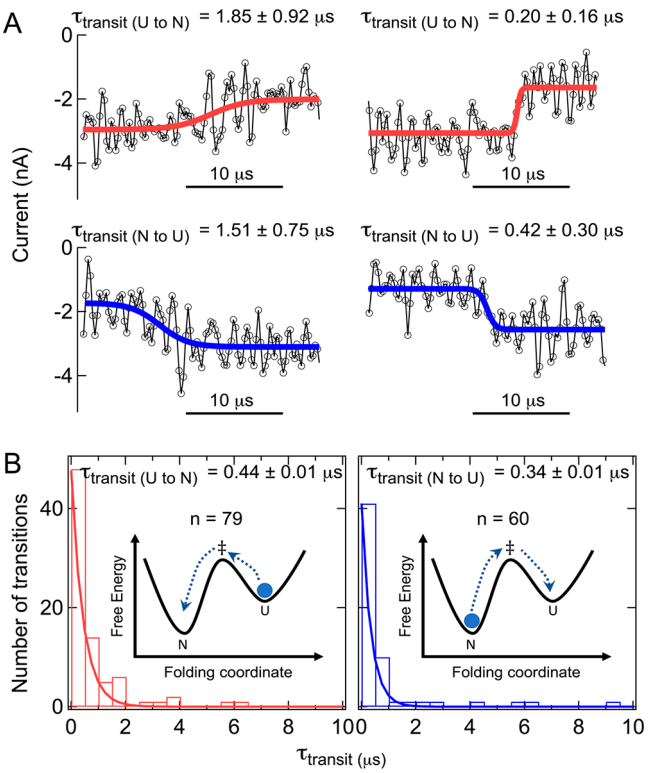


**Figure 2.** Resolving the transition state passage of the N27C mutant between native (N) and unfolded (U) states. (A) Example extracted transitions of U → N (red) and N → U (blue) measured with a 4 nm pore using a custom Chimera instrument with a 4.17 MHz sampling rate at −200 mV and low pass filtered at 2 MHz. The solid curve represents the fit with a sigmoidal function yielding transit time $\tau_{transit}$ between N and U states. (B) Distribution of estimated transition time for U → N transitions and N → U transitions. The red and blue solid lines in (B) and (C) are exponential fits to the data with $\tau \approx 0.4$ μs.

Singular value decomposition analysis (Figure S2) of the distributions of average fractional current blockade ($\Delta I/I_0$) as a function of voltage validated that N27C can be described as a two-state (N ↔ U) protein with 95% accuracy and that the population of the N and U states can be controlled by voltage without the need for chemical denaturants. The scatter plots of $\Delta I/I_0$ vs residence times of the protein at the nanopore for several single-molecule events are shown in Figure S3. At low voltage bias (~200 mV), the vast majority (~99%) of events correspond to protein translocation shortly after the protein settles on the pore because the translocation time of the protein (with pore diameter > protein diameter) at lower voltage bias is shorter than the residence time of the protein in the individual N and U conformational states. However, in ~1% of events ($n$ = 55) we observe transitions in ionic current blockades at rates in the range of ~20000−100000 $s^{-1}$ before translocation restores the open-pore current (see example traces in Figure 1C,D), consistent with the relaxation time observed previously in T-jump experiments.[22] The average rate of arrival of a protein molecule to the pore at −200 mV is <25 $s^{-1}$ (Figure S4), precluding the possibility that the observed rapid transitions in ionic current are due to docking/undocking of a second molecule at the pore mouth. Prior findings[15] indicated that the folded state of a protein blocks the current more in comparison to more solvent- and ion-permeable unfolded state. Thus, observed transitions in ionic current are due to N-to-U and U-to-N transitions before translocation occurs. We extracted these events (see the Methods section in the Supporting Information for the procedure) and used a sigmoidal fitting function to describe the transition state passage dynamics from single-molecule ionic current signals within our signal-to-noise ratio in all cases.[9]

Example N-to-U and U-to-N transitions for the two-state N27C mutant and the fits with a sigmoidal function are shown in Figure 2A and Figure S5. The sigmoidal fits yield separate transition state passage times $\tau_{transit}$ for the forward U → N and backward N → U reaction. For a two-state system, prior theoretical[23] and experimental[13] investigations indicated exponential behavior of transit time distributions at sufficiently long times. A single-exponential fit to the histograms of $\tau_{transit}$ (Figure 2B) yields a similar average transition state passage time for the U → N and N → U transitions, as expected from the principle of microscopic reversibility. However, we note that in ~60% of the total U → N transitions and ~68% of the total N → U transitions the passage times are faster than 0.5 μs, our set bandwidth limit. A significant fraction of N ↔ U transition state passage times are overestimated in our measurements due to the limited time resolution of the data because of the 2 MHz filter (rise time of the instrument at this bandwidth is ~0.25 μs). Nevertheless, our measurements resolve the 30−40% of passage times in the tail of the passage time distribution and suggest that the observed transition state passage reported here at room temperature is faster than the measurement reported for WW domain in ref 9 at a higher temperature (>60 °C) near the melting point of the protein and also somewhat faster than observed for λ-repressor fragment in ensemble experiments at higher temperature (also near the thermal unfolding midpoint).[24] It has been hypothesized previously that lowering the temperature speeds up $\tau_{transit}$ because of reduced hydrophobic sticking of the polypeptide chain at lower temperature,[9] and our present results support this hypothesis through direct observation of faster transition state passage (by about a factor of 4) well


https://doi.org/10.1021/acs.jpclett.2c01009
J. Phys. Chem. Lett. 2022, 13, 5918−5924

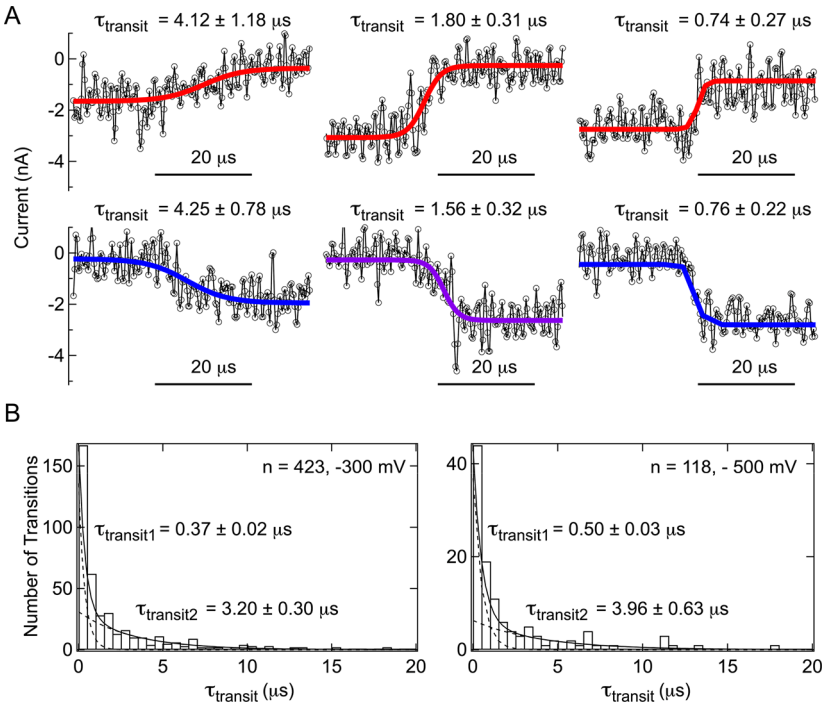


**Figure 3.** Transition state passage of the cytochrome *c* between partially folded metastable intermediates to unfolded states. (A) Example extracted transitions measured with a 3 nm pore using a custom Chimera instrument with a 4.17 MHz sampling rate at −300 mV in 1 M KCl, 0.5 M guanidinium chloride, and 10 mM HEPES buffer and filtered at 2 MHz. The solid curve represents fit with sigmoidal function yielding transit time $\tau_{transit}$ among metastable, intermediate, and unfolded states. (B) Distribution of transition times measured at −300 and −500 mV. The black solid lines in (B) are double-exponential fits to the data yielding two average transition times $\tau_{transit1}$ and $\tau_{transit2}$. The dotted lines represent the individual components of the double-exponential fit.

below the unfolding temperature. An alternative possibility based on Kramers' model is that the curvature of the free energy barrier becomes smaller at a higher temperature, rendering the transition state passage time scales to be longer. This is possible if the unfolded state is less native-like and thus further from the native state along the reaction coordinate.

Previous hydrogen exchange (HX) pulse labeling experiments on cyt *c* reported that its folding and unfolding time scale spans between 1 and 100 ms.[17] The use of a pore of diameter larger than cyt *c* will cause the translocation of the folded protein on a time scale much shorter (<100 $\mu$s) than the lifetime of individual states of cyt *c* and therefore would not allow the observation of transition state passage: proteins would translocate instead of undergoing an equilibrium between native, intermediate, and unfolded states at the pore. As reported previously,[15] the use of a slightly smaller diameter nanopore can extend the translocation time to milliseconds or longer time scales. However, the use of small pores to increase residence time of the protein at the pore also causes a low signal-to-noise ratio of individual protein states at the very high bandwidth of 2 MHz because of the reduced ionic current. Therefore, one needs to have a delicate balance among pore diameter, electrolyte concentration, and voltage bias to observe the transition state dynamics for cyt *c* using a nanopore. Only the use of a nanopore of diameter lightly smaller than cyt *c* and in the presence of a small amount of chemical denaturant such as guanidinium chloride (GdmCl) would make the translocation time at higher voltage bias comparable to the lifetime of individual folded and unfolded protein states to allow observation of the transition state passage.

Thus, to compare the transition state passage time of fast-folding two-state N27C with a slow-folding multistate cyt *c*, we introduced 0.5 M GdmCl in our buffer and applied a higher voltage bias (−300 to −500 mV) using a 3 nm pore so that the individual conformational transitions can be observed. Example ionic current traces for cyt *c* measured at −300 and −500 mV in a buffer solution containing 0.5 M GdmCl are shown in Figure S6. Scatter plots of average current blockade ratio and residence time are shown in Figure S7; these results suggest that the more folded protein state produces deeper and longer current blockade in comparison to the unfolded state. The distribution of current blockage as a function of voltage (Figure S8) suggests that the population of unfolded states increases upon increasing the voltage bias. At −300 mV voltage bias, we found that nearly 10% of the total events contained transitions between different protein states. As described for N27C, we extracted such events and used a sigmoidal function to describe the transition state dynamics from single-molecule ionic current signals.

A few examples of forward and backward single-molecule transitions between different protein states are shown in Figure 3A and Figures S9−S12. The sigmoidal fits of transitions yield the transition state passage time $\tau_{transit}$ between different conformational states at different voltage biases −300 and −500 mV. Histograms of $\tau_{transit}$ measured for unfolding (e.g., N to I) and refolding (e.g., U to I) events show a very similar distribution, again confirming microscopic reversibility for this multistate process when averaged over states. Both histograms of $\tau_{transit}$ at different voltage biases suggest that the transition state passage time distribution is broader than a single-exponential distribution function of times, and at least a biexponential function is needed to fit the data. As shown in


https://doi.org/10.1021/acs.jpclett.2c01009
J. Phys. Chem. Lett. 2022, 13, 5918−5924

Figure 3B, using a double-exponential fit, we found similar time constants at −300 and −500 mV, respectively, suggesting that the transition state dynamics is not coupled to the translocation bias. Thus, the higher bias results for cyt *c* should still report on a field-unperturbed passage time at 0.5 M denaturant.

We found that for ∼40% of the total transitions at −300 mV and ∼37% of the total transitions at −500 mV the transition passage times are shorter than 0.5 $\mu$s, and the remaining >60% are longer than the 0.5 $\mu$s time scale and thus are resolvable. The two time constants 3 and 0.4 $\mu$s obtained from the histogram of $\tau_{transit}$ in Figure 3 correspond to a combination of N−I and I−U events and are close to the 1 $\mu s^{-1}$ "speed limit" inferred from the denatured chain reconfiguration time of cyt *c*.[5] A nonexponential distribution of transition passage time suggests that a 1-D energy surface, by using just one coordinate, is not sufficient to account for the data. In a prior report, by monitoring two different signals (infrared spectroscopy and fluorescence spectroscopy signals), we showed that the fast "molecular phase" due to transition state passage also could not be fitted by a monoexponential distribution.[25] As a more sophisticated approach than Kramers' 1-D analysis, Langevin dynamics on a two-dimensional reaction surface was consistent with the observed nonexponential dynamics.[25] Furthermore, recent theoretical investigations on single-molecule transition path time strongly suggest that the broader than the monoexponential distribution of transition state passage time is a signature of multidimensionality of the free energy landscapes.[26]

To further understand the nature of the distribution of $\tau_{transit}$ for cyt *c* in view of a multidimensional free energy surface, we constructed the histograms of $\tau_{transit}$ and ln $k_{transit}$ (where $k_{transit} = 10^6/\tau_{transit}$ in the unit of seconds) by combining data for the two different −300 and −500 mV voltage biases. We fit the histogram of $\tau_{transit}$ (Figure 4A) to a combined exponential and a stretched exponential ($e^{-(t/\tau)^{\beta}}$), yielding time constants of 0.4 and 1.1 $\mu$s with a stretching exponent power of $\beta = 0.6$. These values are remarkably close to the ensemble fit for the reconfiguration time of cyt *c*,[5] and the stretching exponent fitted for downhill folding of lambda repressor,[25] where a 2-D energy surface was sufficient to reproduce the nonexponential "downhill" kinetics.

To quantitatively analyze the nature of saddle point region in the conformational transitions, we follow the Szabo and Hummer approach where the passage time is related to the diffusion coefficient $D^{\dagger}$ ($m^2/s$) at the barrier top, the curvature $\omega^{\dagger 2}$ of the barrier top, and the temperature as[27]

$$\tau_{TSP} \approx \frac{k_B T}{D^{\dagger}\omega^{\dagger 2}} \ln\left(\frac{2e^{\gamma}\Delta G^{\ddagger}}{k_B T}\right)$$

Here, $\gamma$ is Euler's constant (0.577), $\Delta G^{\ddagger}$ is the free energy barrier separating two conformational states, $k_B$ is Boltzmann's constant, and $T$ is the temperature. If we use a diffusion coefficient for peptide loop closure rate that is consistent in both simulations and experiment,[4,28] $D^{\dagger} \approx 60$ nm$^2/\mu$s and $\Delta G^{\ddagger} = 4.5\ k_B T$, we obtain for the curvature of the barrier top $\omega^{\dagger 2} = 0.28$ kJ mol$^{-1}$ nm$^{-2}$ for the observed $\tau_{TSP} \approx 0.4$ $\mu$s for N27C mutant. On the other hand, using $\Delta G^{\ddagger} = 21\ k_B T$ for cyt *c*, we obtain $\omega^{\dagger 2} = 0.44$ kJ mol$^{-1}$ nm$^{-2}$ and 0.16 kJ mol$^{-1}$ nm$^{-2}$ to obtain the time constants 0.4 and 1.1 $\mu$s in Figure 4A. Using $G = G^{\dagger} - \frac{3}{2}\omega^{\dagger 2}x^2$ for the free energy near the barrier top

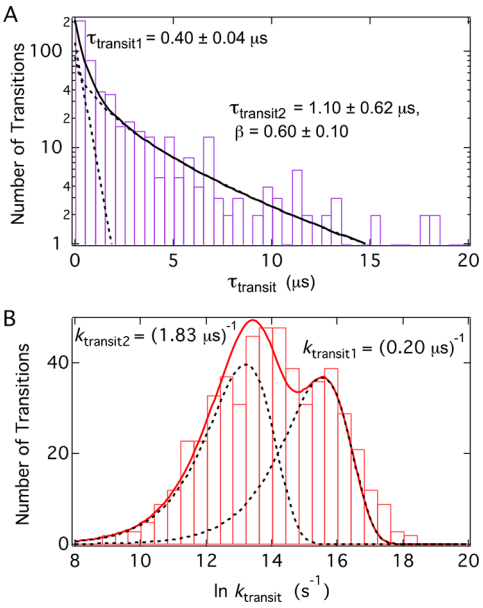


**Figure 4.** Nonexponential transition state passage. (A) Distribution of transition state passage by combining −300 and −500 mV data. The solid curve is fit with a sum of an exponential and a stretched exponential; dotted curves are individual components of the exponential and stretched exponential. (B) Distribution of transit time after converting each time to transit rate ln $k_{transit}$. The solid curve represents a fit with the sum of two exponential upon ln transformation having form $f(x) = a_1(\exp(x - x_{01}) - \exp(x - x_{01})) + a_2(\exp(x - x_{02}) - \exp(x - x_{02}))$, where $x = \ln k_{transit}$.

(including scaling the diffusion coefficient by 1/3 for 1-dimensional diffusion along the reaction coordinate), this corresponds to a rough width of the saddle point region of 2.4 nm for N27C as well as 1.9 nm (corresponds to 0.4 $\mu$s) and 3.2 nm (corresponds to 1.1 $\mu$s) for cyt *c* within 1 $k_B T$ of the top of the barrier when the end-to-end distance is used as a reaction coordinate. These length scales are in the range of radius of gyration for the unfolded states of these proteins and therefore plausible. We note that estimates of the transition state passage time in terms of its inverse, the "molecular rate",[9] have yielded times in the 100 ns−10 $\mu$s range, consistent with loop closure or tertiary structure contact formation as a rate-limiting step. Our results are also consistent with molecular dynamics simulations of transition state passage.[29] Although the viscosity of TIP3P water is too low by about a factor of 3 compared to experiment,[30] MD simulations show that transition state passage for a very similar lambda repressor fragment occurs on the order of ∼1 $\mu$s,[31,29] typical of Type I or Type IIa folders.[10]

Kramers' analysis of a recent force experiment has yielded a much longer passage time for PrP dimer (0.5 ms).[13] Coupled with the resulting very small diffusion coefficient this analysis yielded a folding barrier <1 $kT$ for the reaction (downhill folding), inconsistent with the measured PrP dimer folding time of several seconds.[32] We surmise that PrP dimer instead folds by the type IIB mechanism proposed by Bryngelson et al.:[10] it undergoes a glass transition and progresses very slowly from the unfolded state to the native state. Whether PrP dimer folds downhill or is a type IIB folder, either way Kramers' model using a single barrier-top curvature is not applicable, and PrP is not a typical example of transit times.



https://doi.org/10.1021/acs.jpclett.2c01009
J. Phys. Chem. Lett. 2022, 13, 5918−5924

In summary, we have used here a nanopore-based approach to measure individual protein transition state passage times for two protein molecules: lambda repressor fragment (N27C) and cytochrome *c*. Our high-bandwidth measurements resolve down to submicrosecond transition state passage times and suggest that lowering the temperature speeds up the transition state passage time for N27C, consistent with reduced hydrophobic sticking of the chain to itself or an increase of the curvature of the activation barrier as the unfolded state becomes more native-like. The distribution of transition state passage times for cyt *c* is broader due to the presence of folding intermediate states; it cannot be fitted by a single exponential, consistent with transition state passage on a multidimensional free energy surface. More than half of the observed transition state dynamics is faster than 0.5 $\mu$s, so we were only able to observe the tail of the distribution at room temperature. Further refinements in instrumentation may make almost the entire distribution accessible for a quantitative analysis in the near future.

## ■ ASSOCIATED CONTENT

### Supporting Information

The Supporting Information is available free of charge at https://pubs.acs.org/doi/10.1021/acs.jpclett.2c01009.

Materials and methods, example ionic current traces, additional analysis of single-molecule events such as distribution of current blockade ratio ($\Delta I/I_0$), scatter plots of $\Delta I/I_0$ and residence time ($\tau_{residence}$), additional transition state passage trajectories (PDF)

Transparent Peer Review report available (PDF)

## ■ AUTHOR INFORMATION


### Corresponding Authors

**Martin Gruebele** − *Department of Chemistry, Department of Physics, Center for Biophysics and Quantitative Biology, and Carle-Illinois College of Medicine, University of Illinois at Urbana−Champaign, Urbana, Illinois 61801, United States;* orcid.org/0000-0001-9291-8123; Email: mgruebel@illinois.edu

**Meni Wanunu** − *Department of Physics, Northeastern University, Boston, Massachusetts 02115, United States;* orcid.org/0000-0002-9837-0004; Email: wanunu@neu.edu

### Authors

**Prabhat Tripathi** − *Department of Physics, Northeastern University, Boston, Massachusetts 02115, United States;* orcid.org/0000-0002-9013-2132

**Arash Firouzbakht** − *Department of Chemistry, University of Illinois at Urbana−Champaign, Urbana, Illinois 61801, United States*

Complete contact information is available at: https://pubs.acs.org/10.1021/acs.jpclett.2c01009


### Notes

The authors declare no competing financial interest.

## ■ ACKNOWLEDGMENTS

P.T. and M.W. acknowledge support by the National Institutes of Health (R21HG011689) for this work. M.G. and A.F. acknowledge support by the National Science Foundation (MCB 2205665) for this work.

## ■ REFERENCES


(1) Gelman, H.; Gruebele, M. Fast Protein Folding Kinetics. *Q. Rev. Biophys.* **2014**, *47* (2), 95−142.

(2) Kramers, H. A. Brownian Motion in a Field of Force and the Diffusion Model of Chemical Reactions. *Physica* **1940**, *7* (4), 284−304.

(3) Gruebele, M.; Zewail, A. H. Ultrafast Reaction Dynamics. *Phys. Today* **1990**, *43* (5), 24−33.

(4) Lapidus, L. J.; Eaton, W. A.; Hofrichter, J. Measuring the Rate of Intramolecular Contact Formation in Polypeptides. *Proc. Natl. Acad. Sci. U. S. A.* **2000**, *97* (13), 7220−7225.

(5) Hagen, S. J.; Hofrichter, J.; Szabo, A.; Eaton, W. A. Diffusion-Limited Contact Formation in Unfolded Cytochrome c: Estimating the Maximum Rate of Protein Folding. *Proc. Natl. Acad. Sci. U. S. A.* **1996**, *93* (21), 11615−11617.

(6) Szczepaniak, M.; Iglesias-Bexiga, M.; Cerminara, M.; Sadqi, M.; Sanchez de Medina, C.; Martinez, J. C.; Luque, I.; Muñoz, V. Ultrafast Folding Kinetics of WW Domains Reveal How the Amino Acid Sequence Determines the Speed Limit to Protein Folding. *Proc. Natl. Acad. Sci. U. S. A.* **2019**, *116* (17), 8137−8142.

(7) Chandler, D.; Percus, J. K. Introduction to Modern Statistical Mechanics. *Phys. Today* **1988**, *41* (12), 114−118.

(8) Yang, W. Y.; Gruebele, M. Folding at the Speed Limit. *Nature* **2003**, *423* (6936), 193−197.

(9) Liu, F.; Nakaema, M.; Gruebele, M. The Transition State Transit Time of WW Domain Folding Is Controlled by Energy Landscape Roughness. *J. Chem. Phys.* **2009**, *131* (19), 195101.

(10) Bryngelson, J. D.; Onuchic, J. N.; Socci, N. D.; Wolynes, P. G. Funnels, Pathways, and the Energy Landscape of Protein Folding: A Synthesis. *Proteins: Struct., Funct., Bioinf.* **1995**, *21* (3), 167−195.

(11) Liu, F.; Du, D.; Fuller, A. A.; Davoren, J. E.; Wipf, P.; Kelly, J. W.; Gruebele, M. An Experimental Survey of the Transition between Two-State and Downhill Protein Folding Scenarios. *Proc. Natl. Acad. Sci. U. S. A.* **2008**, *105* (7), 2369−2374.

(12) Chung, H. S.; McHale, K.; Louis, J. M.; Eaton, W. A. Single-Molecule Fluorescence Experiments Determine Protein Folding Transition Path Times. *Science* **2012**, *335* (6071), 981−984.

(13) Neupane, K.; Foster, D. A. N.; Dee, D. R.; Yu, H.; Wang, F.; Woodside, M. T. Direct Observation of Transition Paths during the Folding of Proteins and Nucleic Acids. *Science* **2016**, *352* (6282), 239−242.

(14) Chung, H. S.; Eaton, W. A. Protein Folding Transition Path Times from Single Molecule FRET. *Curr. Opin. Struct. Biol.* **2018**, *48*, 30−39.

(15) Tripathi, P.; Benabbas, A.; Mehrafrooz, B.; Yamazaki, H.; Aksimentiev, A.; Champion, P. M.; Wanunu, M. Electrical Unfolding of Cytochrome *c* during Translocation through a Nanopore Constriction. *Proc. Natl. Acad. Sci. U. S. A.* **2021**, *118* (17), No. e2016262118.

(16) Yang, W. Y.; Gruebele, M. Rate-Temperature Relationships in $\lambda$-Repressor Fragment $\lambda_{6-85}$ Folding †. *Biochemistry* **2004**, *43* (41), 13018−13025.

(17) Hu, W.; Kan, Z.-Y.; Mayne, L.; Englander, S. W. Cytochrome *c* Folds through Foldon-Dependent Native-like Intermediates in an Ordered Pathway. *Proc. Natl. Acad. Sci. U. S. A.* **2016**, *113* (14), 3809−3814.

(18) Larkin, J.; Henley, R. Y.; Muthukumar, M.; Rosenstein, J. K.; Wanunu, M. High-Bandwidth Protein Analysis Using Solid-State Nanopores. *Biophys. J.* **2014**, *106* (3), 696−704.

(19) Rosenstein, J. K.; Wanunu, M.; Merchant, C. A.; Drndic, M.; Shepard, K. L. Integrated Nanopore Sensing Platform with Sub-Microsecond Temporal Resolution. *Nat. Methods* **2012**, *9* (5), 487−492.

(20) Kim, M. J.; Wanunu, M.; Bell, D. C.; Meller, A. Rapid Fabrication of Uniformly Sized Nanopores and Nanopore Arrays for Parallel DNA Analysis. *Adv. Mater.* **2006**, *18* (23), 3149−3153.

(21) Huang, G. S.; Oas, T. G. Submillisecond Folding of Monomeric Lambda Repressor. *Proc. Natl. Acad. Sci. U. S. A.* **1995**, *92* (15), 6878−6882.

(22) Chao, S.-H.; Schäfer, J.; Gruebele, M. The Surface of Protein $\lambda_{6-85}$ Can Act as a Template for Recurring Poly(Ethylene Glycol) Structure. *Biochemistry* **2017**, *56* (42), 5671−5678.
(23) Chaudhury, S.; Makarov, D. E. A Harmonic Transition State Approximation for the Duration of Reactive Events in Complex Molecular Rearrangements. *J. Chem. Phys.* **2010**, *133* (3), 034118.
(24) Yang, W. Y.; Gruebele, M. Folding λ-Repressor at Its Speed Limit. *Biophys. J.* **2004**, *87* (1), 596−608.
(25) Ma, H.; Gruebele, M. Kinetics Are Probe-Dependent during Downhill Folding of an Engineered $\lambda_{6-85}$ Protein. *Proc. Natl. Acad. Sci. U. S. A.* **2005**, *102* (7), 2283−2287.
(26) Satija, R.; Berezhkovskii, A. M.; Makarov, D. E. Broad Distributions of Transition-Path Times Are Fingerprints of Multidimensionality of the Underlying Free Energy Landscapes. *Proc. Natl. Acad. Sci. U. S. A.* **2020**, *117* (44), 27116−27123.
(27) Hummer, G. From Transition Paths to Transition States and Rate Coefficients. *J. Chem. Phys.* **2004**, *120* (2), 516−523.
(28) Portman, J. J. Non-Gaussian Dynamics from a Simulation of a Short Peptide: Loop Closure Rates and Effective Diffusion Coefficients. *J. Chem. Phys.* **2003**, *118* (5), 2381−2391.
(29) Lindorff-Larsen, K.; Piana, S.; Dror, R. O.; Shaw, D. E. How Fast-Folding Proteins Fold. *Science* **2011**, *334* (6055), 517−520.
(30) Venable, R. M.; Hatcher, E.; Guvench, O.; MacKerell, A. D.; Pastor, R. W. Comparing Simulated and Experimental Translation and Rotation Constants: Range of Validity for Viscosity Scaling. *J. Phys. Chem. B* **2010**, *114* (39), 12501−12507.
(31) Liu, Y.; Prigozhin, M. B.; Schulten, K.; Gruebele, M. Observation of Complete Pressure-Jump Protein Refolding in Molecular Dynamics Simulation and Experiment. *J. Am. Chem. Soc.* **2014**, *136* (11), 4265−4272.
(32) Yu, H.; Dee, D. R.; Liu, X.; Brigley, A. M.; Sosova, I.; Woodside, M. T. Protein Misfolding Occurs by Slow Diffusion across Multiple Barriers in a Rough Energy Landscape. *Proc. Natl. Acad. Sci. U. S. A.* **2015**, *112* (27), 8308−8313.


https://doi.org/10.1021/acs.jpclett.2c01009
*J. Phys. Chem. Lett.* 2022, 13, 5918−5924